Pharmaceutical Research, Vol. 22, No. 6, June 2005 (© 2005)
DOI: 10.1007/s11095-005-4581-4

Research Paper

Formulating Paclitaxel in Nanoparticles Alters Its Disposition

Teng Kuang Yeh,[1,3] Ze Lu,[1,3] M. Guillaume Wientjes,[1,2] and Jessie L.-S. Au[1,2,4]

Received December 9, 2004; accepted February 17, 2005

Purpose. Paclitaxel is active and widely used to treat multiple types of solid tumors. The commercially available paclitaxel formulation uses Cremophor/ethanol (C/E) as the solubilizers. Other formulations including nanoparticles have been introduced. This study evaluated the effects of nanoparticle formulation of paclitaxel on its tissue distribution.
Methods. We compared the plasma and tissue pharmacokinetics of paclitaxel-loaded gelatin nanoparticles and the C/E formulation. Mice were given paclitaxel-equivalent doses of 10 mg/kg by intravenous injection.
Results. The nanoparticle and C/E formulations showed significant differences in paclitaxel disposition; the nanoparticles yielded 40% smaller area under the blood concentration-time curve and faster blood clearance of total paclitaxel concentrations (sum of free, protein-bound, and nanoparticle-entrapped drug). The two formulations also showed different tissue specificity. The rank order of tissue-to-blood concentration ratios was liver > small intestine > kidney >> large intestine > spleen = stomach > lung > heart for the nanoparticles, and liver > small intestine > large intestine > stomach > lung ≥ kidney > spleen > heart for the C/E formulation. The nanoparticles also showed longer retention and higher accumulation in organs and tissues (average of 3.2 ± 2.3-fold), especially in the liver, small intestine, and kidney. The most striking difference was an 8-fold greater drug accumulation and sustained retention in the kidney.
Conclusions. These data indicate that formulation of paclitaxel affects its clearance and distribution into tissues, with preferential accumulation of nanoparticles in the liver, spleen, small intestine, and kidney.

KEY WORDS: cremophor; formulation; gelatin nanoparticles; paclitaxel; tissue distribution.

INTRODUCTION

Paclitaxel is one of the most important anticancer drugs developed in the past two decades, with significant antitumor activity against ovarian, head and neck, bladder, breast, and lung cancers (1). Paclitaxel promotes microtubule assembly and stabilizes microtubule dynamics, resulting in inhibition of cell proliferation and induction of apoptosis (2).

Paclitaxel has a low aqueous solubility. In the commercially available formulation, paclitaxel is solubilized in a mixture of Cremophor EL (polyoxyethylated castor oil) and ethanol (1:1, w/w) (C/E formulation). Intravenous administration of this formulation resulted in peak paclitaxel concentration in plasma at the first sampling time, followed by biphasic declines over time (3). Paclitaxel disposition is nonlinear, in part due to the presence of Cremophor (4,5). Hepatic metabolism and biliary excretion are the main elimination pathways for the C/E formulation (6,7). The dose-limiting toxicity of paclitaxel is neutropenia, which is related to the duration of time that plasma paclitaxel concentrations are at or above a threshold value (0.05 μM) and not directly related to the peak plasma concentration and the area under the plasma concentration-time curve of paclitaxel (4,5). The use of Cremophor is also associated with hypersensitivity reactions (8). Sequestration of paclitaxel into Cremophor micelles results in reduction in the free fraction of paclitaxel and consequently the penetration across epithelium (9). These concerns have motivated significant efforts to reformulate paclitaxel, in the hope of finding a formulation with greater antitumor activity and reduced toxicity. In a new formulation, ABI-007, paclitaxel molecules are bound to and/or coated with human serum albumin, resulting in particles with a mean particle diameter of 120–150 nm (10,11). ABI-007 shows a higher activity in breast cancer patients as compared with the C/E formulation (12), and its plasma pharmacokinetics in patients has been reported (13). A preliminary preclinical study reported in 2000 suggested different disposition and/or tissue distribution as mechanisms of the different activity of the C/E and nanoparticles formulations (14), but a full report on tissue distribution is not available.

[1] College of Pharmacy, The Ohio State University, Columbus, Ohio, USA.
[2] James Cancer Hospital and Solove Research Institute, The Ohio State University, Columbus, Ohio, USA.
[3] Present address: Optimum Therapeutics LLC, OSU Science Tech Village, Columbus, Ohio, USA.
[4] To whom correspondence should be addressed. (e-mail: au.1@osu.edu)

ABBREVIATIONS: AUC, area under concentration-time curve; C/E, Cremophor/ethanol; CL, clearance; HPLC, high-performance liquid chromatography; RES, reticuloendothelial system.

The current study evaluated the effect of formulating paclitaxel in nanoparticles on its tissue distribution by comparing the blood/plasma and tissue pharmacokinetics of paclitaxel-loaded gelatin nanoparticles and the C/E paclitaxel formulation.

MATERIALS AND METHODS

Chemicals and Reagents

Gelatin type A from porcine skin (175 bloom), glutaraldehyde (25%, w/v in water), Sephadex G-50 m, Tween 20 (polysorbate 20, polyoxyethylene sorbitan monolaurate), sodium sulfate, sodium metabisulfite, and isopropanol were purchased from Sigma Chemical Company (St. Louis, MO, USA). Paclitaxel was purchased from Yunnan Tech Development Co. Ltd. (Jinching, China). The C/E paclitaxel formulation (i.e., Taxol) was purchased from Bristol-Myers Squibb Co. (Princeton, NJ, USA). Cephalomannine was supplied by the National Cancer Institute (Bethesda, MD, USA). Chemicals and solvents used for high-performance liquid chromatography (HPLC) and to prepare anesthetics were of the highest available grades and purchased from Fisher Scientific Company (Fair Lawn, NJ, USA). HPLC analysis showed that paclitaxel and cephalomannine were >99% pure. All chemicals and reagents were used as received.

Preparation of Paclitaxel-Loaded Nanoparticles

Gelatin was used as the polymeric coating agent because of its biocompatibility; gelatin is widely used as a stabilizer in vaccines and has been approved by the U.S. FDA for extravascular administration (15). The preparation and characterization of paclitaxel-loaded gelatin nanoparticles are described elsewhere (16). Briefly, the nanoparticles were prepared according to the coacervation-phase separation method of Oppenheim *et al.*, with some modifications (17,18). Gelatin was dissolved in 10 ml water containing 2% Tween 20. The solution was heated to 40°C with constant stirring at 300 rpm. To this solution, 2 ml of a 20% aqueous solution of sodium sulfate was added slowly, followed by 1 ml isopropanol containing paclitaxel. A second aliquot of sodium sulfate solution (5.5–6 ml) was added until the solution turned turbid, which indicated the formation of gelatin aggregates. Approximately 1 ml distilled water was then added until the solution turned clear. Aqueous solution of glutaraldehyde (25%, 0.4 ml) was added to cross-link the gelatin. Sodium metabisulfite solution (12%, 5 ml) was added 5 min later to stop the cross-linking process. After 1 h, the crude product was purified on a Sephadex G-50 column. The nanoparticle-containing fraction was lyophilized in a freeze dryer over 48 h. The drug content in the paclitaxel-loaded gelatin nanoparticles, determined after enzymatic digestion using a proteolytic enzyme, pronase (Sigma), was 2%. The diameter of the nanoparticles, determined using scanning electron microscopy, ranged from 300 to 900 nm, with a mean value of 664 nm and a median value of 648 nm. The entrapment efficiency of paclitaxel, calculated as the ratio of (drug concentration in nanoparticles) to (amount of drug added to blank nanoparticles), was 70%. Degradation of the paclitaxel-loaded gelatin nanoparticles as a suspension (dissolved in phosphate-buffered physiologic saline with a pH of 7.4 or distilled water) was 20% after 96 h at 37°C, less than 10% after 120 h at room temperature and less than 2% after 6 months when stored at −4°C. Drug release from nanoparticles was rapid with more than 55%, 87%, and 92% released in phosphate-buffered saline at 37°C, after 15 min, 2 h, and 3 h, respectively (16).

Animal Protocol

Female Balb/c nude mice (Charles River, Wilmington, MA, USA), 5–6 weeks old, were housed in metabolic cages (5 mice/cage) and had access to food and water *ad libitum*. Animals were cared for according to institutional guidelines. The pretreatment body weights of the mice were 18 ± 2 g.

A mouse was anesthetized with an intraperitoneal injection of Avertin (2.5 g of 2,2,2-tribromoethanol and 5 ml of *tert*-amyl alcohol, diluted with 500 ml 0.9% sodium chloride, 300–400 μl per mouse). A paclitaxel-containing solution or suspension was then administered intravenously over 1 min via the tail vein (maximum volume of less than 400 μl). Animals were allowed to regain consciousness, which typically occurred within 30 min. At predetermined time points, a mouse was again anesthetized with Avertin, and the abdomen was opened by midline incision, a blood sample was collected from the ocular artery, and tissues (liver, spleen, lung, heart, kidneys, stomach, small intestine, and large intestine) were excised. The time interval between obtaining the blood sample and the tissue samples was about 2 min. The contents of the gastrointestinal tract were obtained by flushing the lumen with 6 ml of physiologic saline. The flushed intestines and other tissues were blot-dried and weighed. Preliminary data showed that the blood concentrations were at least several-fold lower compared to tissue concentrations. Hence, no attempts were made to remove the residual blood in organs. Blood and tissue samples were kept on ice during processing and subsequently frozen and stored at −70°C until analysis. Three animals were used per time point.

The two formulations were diluted with physiological saline to a concentration of 1 mg/ml, and a dose of 10 mg/kg paclitaxel was administered. As the nanoparticle solution had a high viscosity, we measured the residual amount of nanoparticles in the tail in order to determine the rate of dose input into the systemic circulation. The results showed that 76%, 79%, 87%, 92%, and >99% of the dose was cleared at 5, 10, 60, 180, 300, and 1440 min, respectively.

Extraction and HPLC Analysis of Paclitaxel

Blood and tissue samples were extracted as described previously (19) with some modifications. In brief, 100 μl of blood was mixed with 50 μl of the internal standard (cephalomannine, 20 μg/ml), and extracted with 3 ml of ethyl acetate twice. Frozen tissue samples were mixed with 50 μl of internal standard (ceplalomannine, 20 μg/ml) and homogenized twice in 3 ml ethyl acetate using a rotor-stator type homogenizer (BioSpec Products Inc, Bartlesville, OK, USA). The ethyl acetate fractions were combined and evaporated to dryness. The residue was reconstituted with the HPLC mobile phase and analyzed with our previously reported column-switching HPLC assay (19). The HPLC stationary

phase consisted of a clean-up column (Novapak C_8, 75 × 3.9 mm ID, 4-μm particle size, Waters Associates, Milford, MA, USA) and an analytical column (Bakerbond C_{18}, 250 × 4.6 mm ID, 5 μm particle size from I.D. Baker, Phillipsburg, NJ, USA). Samples were injected onto the clean-up column and eluted with clean-up mobile phase consisting of 37.5% acetonitrile in water at a flow rate of 1 ml/min. Concurrently, the analytical mobile phase consisting of 49% acetonitrile was directed through the analytical column at a flow rate of 1.2 ml/min. The fraction from 8 to 15 min containing paclitaxel and cephalomannine was transferred from the clean-up column onto the analytical column. The limit of sensitivity for paclitaxel was 1 ng per injection, or 14 ng/ml for blood and 40 ng/g for tissue homogenates and intestinal contents.

Determination of Blood-to-Plasma Ratio of Paclitaxel

Two milliliters of fresh heparinized mouse blood was placed in a shaker at 37°C for 15 min together with paclitaxel-loaded gelatin nanoparticles or paclitaxel dissolved in methanol (total concentration of 20 μg/ml). A pilot study indicated that drug concentration between whole blood and plasma reached an equilibrium at 10 min. Subsequent experiments used 15 min incubation. After incubation, aliquots of 100 μl were withdrawn and placed in a −70°C freezer for 5 min to achieve complete hemolysis. The remaining blood was centrifuged, and the supernatant plasma fraction was obtained. The hemolyzed blood and plasma samples were extracted with ethyl acetate and analyzed by HPLC.

Data Analysis

The concentration-time curves of paclitaxel were analyzed using noncompartmental methods. The areas under the curves (AUCs) were calculated using the linear trapezoidal rule. For tissues that showed detectable concentrations throughout the 24-h study period, the AUC was calculated using actual data points from time zero to 24 h (AUC_{0-24}). For tissues that showed undetectable levels at 6 or 24 h, the lower limit of detection was entered as the maximal concentration and used to calculate the upper limits of the AUC_{0-24}. In all cases, the AUCs determined using measured concentrations up to 6 h were greater than 82% of AUC_{0-24}. The blood clearance was calculated as (Dose) divided by (AUC_{0-24}). The volume of distribution at steady state (VD_{ss}) was calculated as (Dose) multiplied by (area under the first moment plasma concentration-time curve) divided by $(AUC_{0-24})^2$. We did not use $AUC_{0-\infty}$ to calculate clearance because the terminal slope was at times ill-defined.

RESULTS

Unequal Blood-to-Plasma Distribution of Paclitaxel Derived from the Gelatin Nanoparticle Formulation

The methanolic paclitaxel showed a blood-to-plasma concentration ratio of 1.00 ± 0.02 (n = 3), indicating equal distribution in plasma and red blood cells. In contrast, the nanoparticles showed a significantly lower ratio of 0.65 ± 0.03 (n = 3, $p < 0.05$), indicating preferential localization of nanoparticles in extracellular fluid relative to blood cells. To avoid potential complication due to concentration- or time-dependent changes in blood-to-plasma ratios, subsequent studies used drug concentrations in whole blood instead of plasma.

Comparison of Blood Pharmacokinetics of Paclitaxel-Equivalents Derived from Gelatin Nanoparticle and Cremophor/Ethanol Formulations

Figure 1 shows the semilogarithmic plots of total paclitaxel concentration in blood (i.e., sum of free, protein-bound, Cremophor micelles-entrapped and/or nanoparticle-entrapped drug) *vs.* time, after administration of the two formulations. As discussed in "Materials and Methods," the high viscosity of nanoparticles resulted in a dose input of ~90% over 1 h, as opposed to the input rate of 100% over 1 min for the C/E formulation. This difference in dose input rate resulted in different times to reach maximal blood concentrations for the two formulations; the C/E formulation showed the highest concentration at the first sampling time point of 5 min, whereas the nanoparticles showed a peak concentration at 10 min. In addition, while both formulations showed biphasic blood concentration decline during subsequent time points, the rates of declines were vastly different. The nanoparticles showed a rapid initial decline to about 2% of the peak level at 1 h followed by a slow decline until 6 h, where concentrations approach the limit of detection. The profile for the C/E formulation showed a much slower decline over the first hour followed by a more rapid decline such that the concentration fell below the detection limit of 14 ng/ml at 6 h. The estimated terminal half-lives were 1.94 and 33.8 h for the C/E formulation and nanoparticles, respectively. The nanoparticles showed a 40% lower AUC_{0-24} in blood (Table I) and consequently a 40% higher blood clearance (2.09 *vs.* 1.49 L h^{-1} kg^{-1}). The volume of distribution at steady state for nanoparticles is 0.046 and 0.53 L for the C/E formulation and nanoparticles, respectively. Note that these parameters were calculated using the averaged values obtained from three mice at each time points.

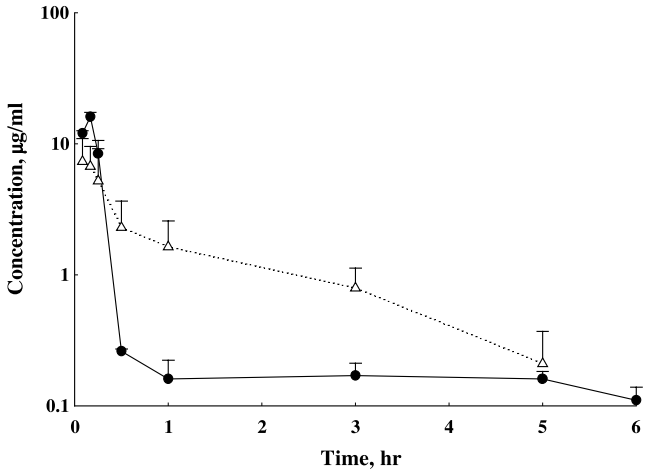

Fig. 1. Effect of paclitaxel formulation on blood concentration-time profiles. Mice were given an intravenous injection of 10 mg/kg paclitaxel-loaded gelatin nanoparticles (solid circles) or paclitaxel solubilized in Cremophor/ethanol (open triangles). Mean ± SD of total paclitaxel concentrations (i.e., free, protein-bound, Cremophor micelle- and/or nanoparticle-entrapped drug).

Table I. Blood and Tissue Pharmacokinetics of Paclitaxel Delivered by Gelatin Nanoparticle and C/E Formulations

	Blood	Lung	Heart	Stomach	Large intestine	Liver	Spleen	Small intestine	Kidney
Nanoparticles									
AUC_{0-24} (μg·h per ml or g)	4.79	36.1	18.6	65.8	75.0	379	64.8	288	165
C_{tissue}:C_{blood} ratio	1.00	6.87	2.89	11.9	21.3	67.0	12.5	59.3	30.3
AUC_{tissue}:AUC_{blood} ratio	1.00	7.53	3.88	13.7	15.7	79.1	13.5	60.1	34.4
C/E formulation									
AUC_{0-24} (μg·h per ml or g)	<6.73	<33.8	<16.0	55.0	88.6	164	>31.9	120	<33.7
C_{tissue}:C_{blood} ratio	1.00	4.20	1.76	6.78	9.8	21.9	2.93	10.5	3.23
AUC_{tissue}:AUC_{blood} ratio	1.00	5.02	2.74	8.17	13.2	24.4	4.74	17.8	5.0
Nanoparticle-to-C/E ratios									
AUC_{0-24} (μg·h per ml or g)	>0.71	>1.1	>1.2	1.2	0.84	2.3	>2.0	2.4	>4.9
C_{tissue}:C_{blood} ratio	1.00	1.64	1.64	1.76	2.17	3.06	4.27	5.65	9.38
AUC_{tissue}:AUC_{blood} ratio	1.00	1.50	1.63	1.68	1.19	3.25	2.85	3.37	6.88

Mice were given an intravenous dose (10 mg/kg paclitaxel-equivalents) of paclitaxel-loaded nanoparticles or paclitaxel dissolved in C/E. AUCs from time zero to 24 h (AUC_{0-24}) were calculated as described in "Materials and Methods." For tissues that showed levels below the detection limits (14 ng/ml for blood and 40 ng/g for tissues), we used the detection limit as the upper limit of concentration at 24 h to calculate the AUC_{0-24}. In all cases, the AUC_{0-6} accounted for >82% of AUC_{0-24}. Hence, potential errors to the approximation of AUC_{6-24} are considered minimal. The C_{tissue}:C_{blood} ratio was the average value of all nine time points. Note that these parameters were calculated using the average data of three mice per time point.

Comparison of Tissue Pharmacokinetics of Paclitaxel-Equivalents Derived from Gelatin Nanoparticle and Cremophor/Ethanol Formulations

Figure 2 shows the concentration-time profiles of total paclitaxel concentrations in tissues. Table I summarizes the half-lives, AUCs in tissues, and the tissue-to-blood concentration ratios and AUC ratios.

For both formulations, the tissue concentrations approached the blood concentrations within 15 min after dose administration and either continued to rise or remained relatively constant for up to 6 h, followed by a slow decline. As blood concentrations declined at a more rapid rate, tissue concentrations exceeded the blood concentrations by up to 333-fold, starting at 1 h.

The two formulations yielded different tissue concentrations. The lung and heart showed higher paclitaxel concentrations for the C/E formulation during the initial 3 h, followed by a crossover with higher concentrations for the nanoparticles during the subsequent time points. In contrast, the remaining tissues showed comparable or higher concentrations for the nanoparticles throughout the entire 24 h experimentation. The most striking difference is the persistent and much higher concentrations in the kidney for the nanoparticles, such that the concentration at 24 h in the kidney accounted for 0.55% of the dose. In contrast, the paclitaxel concentrations were not measurable in kidney tissue at 24 h after C/E administration.

The C/E formulation yielded peak concentrations at the first sampling time of 5 min in the nongastrointestinal tissues (heart, lung, liver spleen, and kidney), and later peak times for stomach and small and large intestines. For the nanoparticles, only the kidney showed the peak concentration at 5 min and all other tissues showed later peak times. In general, total paclitaxel concentrations in tissues derived from the nanoparticles showed a zigzag pattern, initially increasing to reach the first peak within 10 min, then declining and again rising to reach the second peak at 30 min. The concentration of the second peak was on average 195% (range, 60–478%) of the first peak level.

The rates of tissue concentration decline over time were generally slower for the nanoparticles. For example, for the C/E formulation, the concentration decline from 1 to 24 h was 218-fold in lung, 83-fold in small intestine, and at least 55- and 110-fold in heart and kidney (concentrations in heart and kidney were below the limit of detection of 40 ng/g at 24 h). In contrast, for the nanoparticles, the concentrations in all tissues declined by less than 2-to 10-fold and remained 16- to 258-fold above the limit of detection at 24 h.

As shown in Table I, the partitioning from blood to tissue, indicated by the tissue-to-blood concentration ratios, was higher for the nanoparticles compared to the C/E formulation. There are also differences in tissue specificity, as reflected by the differences in the rank order of tissue-to-blood concentration ratios and AUC_{tissue}:AUC_{blood} ratios; that is, liver > small intestine > kidney >> large intestine > spleen ~ stomach > lung > heart for the nanoparticles and liver > small intestine > large intestine > stomach > lung ≥ kidney > spleen > heart for the C/E formulation.

Mass Balance

We calculated the amounts of unchanged paclitaxel in individual tissues as the product of (tissue concentration) and (tissue weight). The amount in blood was calculated using a blood volume of 1.7 ml per 20 g mice (or 1.53 ml for the 18 g mice used in the current study) (20). Figure 3A shows the total dose fractions recovered in intestinal washing as unchanged paclitaxel over time. The nanoparticles showed higher recoveries compared to the C/E formulation at all time points (mean ± SD of 32.3 ± 17.5% *vs.* 23.6 ± 16.6 %; range, 8.1–61.9% *vs.* 2.8–52.3%, respectively).

Figure 3B shows the dose fractions of unchanged drug appearing in the intestinal washing. The excretion of the nanoparticle-derived paclitaxel into the intestinal lumen was rapid; more than 50% of the dose was recovered in the intestinal washing at 1 h and the dose fraction remained relatively constant at ~40% over the 24 h study period. In comparison, the C/E formulation yielded lower dose fractions (average of 2%) during the first hour and reached a lower

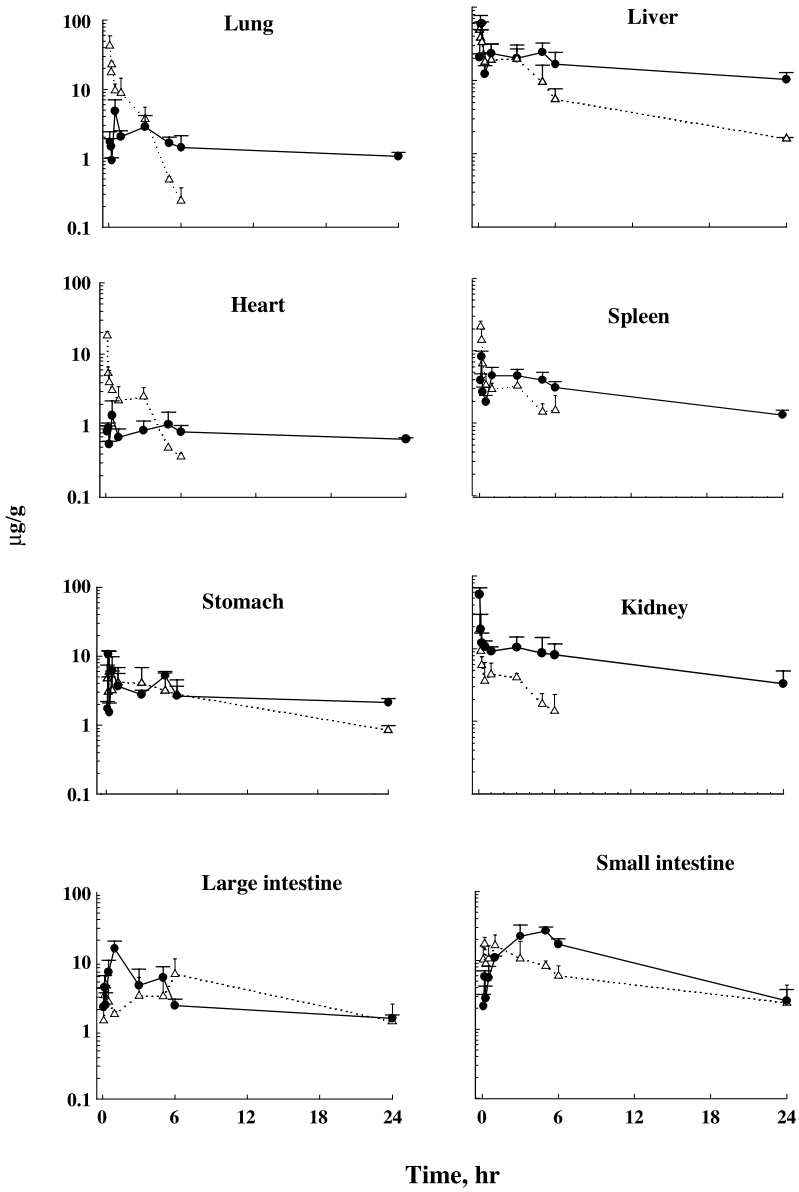

Fig. 2. Effect of formulation on paclitaxel distribution in tissues. Mice were given an intravenous injection of 10 mg/kg paclitaxel-loaded gelatin nanoparticles (solid circles) or paclitaxel solubilized in Cremophor/ethanol (open triangles), and tissues were harvested. Mean ± SD of total paclitaxel concentrations (i.e., free, protein-bound, Cremophor micelle- and/or nanoparticle-entrapped drug).

peak level of ~30% at a later time of 3 h. Likewise, the sums of the dose fractions recovered in tissues plus intestinal washing were higher for the nanoparticles (average of 63% *vs.* 37%; range, 40–85% *vs.* 4.8–57%; Fig. 3C).

DISCUSSION

Uptake and Accumulation of Paclitaxel in Tissues

Our results show that regardless of the formulation, paclitaxel was rapidly and widely distributed in the body, with greater-than-unity tissue-to-blood concentration ratios. These findings are in agreement with the tissue distribution of radiolabeled paclitaxel dissolved in dimethyl sulfoxide or C/E (21,22), and suggest drug accumulation and localization in tissues due to extensive binding (e.g., to intracellular macromolecules) (2,23).

Tissue Distribution of Paclitaxel-Loaded Gelatin Nanoparticles

We studied tissues that are enriched with the reticulo-endothelial (RES) system (i.e., liver, spleen, lungs) and non-RES organs (heart, kidneys, stomach, small intestine, large intestine). Highest drug concentrations were found in liver, small and large intestines, and kidney. The localization of paclitaxel nanoparticles in the liver and lungs is consistent with the uptake by the RES; particulates with an average size

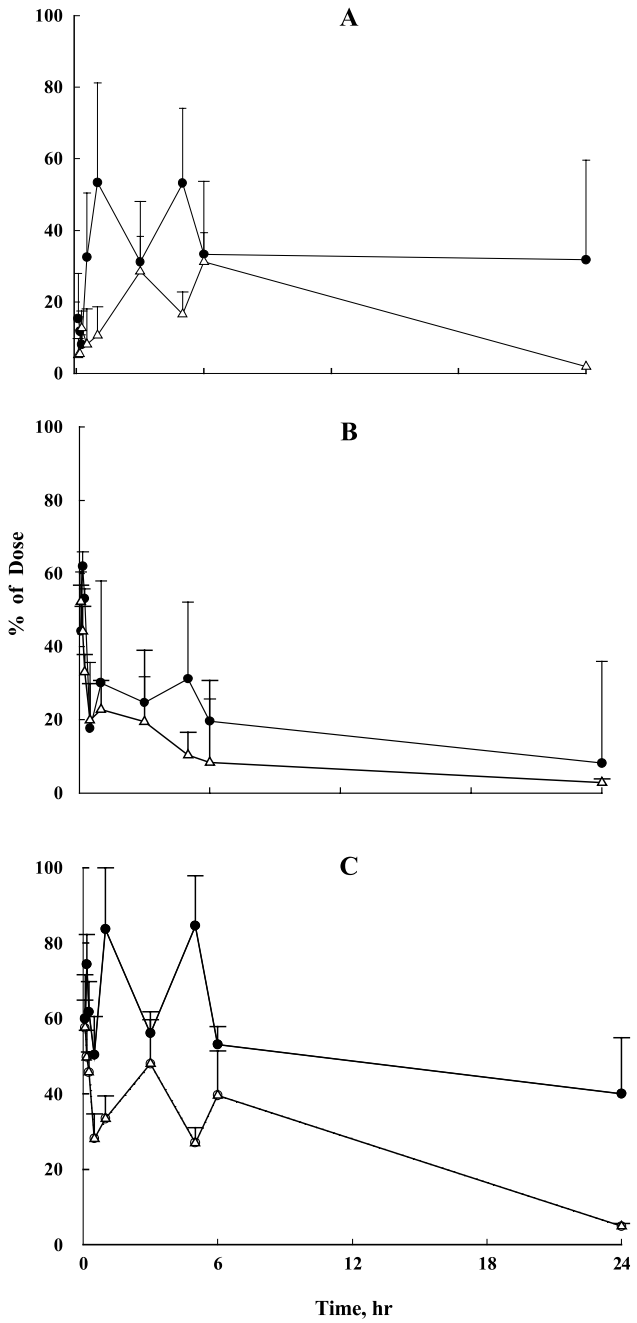

Fig. 3. Mass balance. Mice were given an intravenous injection of 10 mg/kg paclitaxel-loaded gelatin nanoparticles (solid circles) or paclitaxel solublized in Cremophor/ethanol (open triangles). Amounts of total paclitaxel (i.e., free, protein-bound, Cremophor micelle- and/or nanoparticle-entrapped drug) in tissues expressed as a fraction of administered dose in intestinal contents (A), in all other collected tissues (B), and as sums of data in panels A and B (C) (mean ± SD).

below 7 μm are generally taken up by the Kupffer cells in liver (24,25), and gelatin nanoparticles are phagocytosed by RES or taken up by alveolar macrophages in the lungs (26,27). However, the drug concentration in several non-RES organs (small and large intestines, kidney) were several-fold higher compared to major RES organs such as spleen and liver, suggesting that factors other than the RES system also determine the tissue specificity of the nanoparticles.

We also observed differences in times-to-reach-peak-concentrations in various tissues. For example, the kidney showed the shortest whereas the small intestines showed the longest times-to-reach-peak concentrations. Possible causes include differences in the delivery of paclitaxel-loaded gelatin nanoparticles through the vasculature and/or differences in the residence of nanoparticles in tissues. The delayed peak time and the appearance of multiple peaks of paclitaxel concentrations in the intestinal tissues may be due to excretion of paclitaxel into the gastrointestinal tract and the subsequent enterohepatic recirculation (28).

To determine whether collection of drug-containing in urine in the kidney tubules contributed to the high drug accumulation and retention in the kidney, the following calculation was performed. In mice, ~0.26% of an intravenous dose of the C/E paclitaxel formulation is excreted in urine in 96 h (21). The renal clearance calculated using the blood clearance of 2.09 L h^{-1} kg^{-1} found in the current study is therefore 0.005 L h^{-1} kg^{-1}. Hence, the urine concentration, calculated as (blood concentration) × (renal clearance) ÷ (urine flow rate) with an average urine flow rate of 2.08 L h^{-1} kg^{-1} (20,29), is approximately 2.6 times the blood concentration and is significantly lower compared to the observed kidney-to-blood ratio of about 30. This, in turn, rules out urine collection in the kidney as a major cause of the high drug/nanoparticle accumulation and suggests a kidney-targeting effect of the gelatin nanoparticles.

Effect of Paclitaxel Formulation on Its Disposition

Comparisons of paclitaxel disposition indicate several qualitative and quantitative differences in the rate and extent of tissue distribution of paclitaxel formulated in gelatin nanoparticle or C/E. First, the distribution of the C/E formulation from blood to all nongastrointestinal tissues (lung, heart, liver, spleen, kidney) was rapid, as indicated by the early concentration peak time (5 min or the earliest sampling time). In comparison, similarly rapid distribution of nanoparticles was observed only in the kidney, whereas all other nonintestinal tissues showed later peak times. Further, the C/E formulation showed a single peak concentration in tissues, consistent with first-order transfer of a single moiety. In contrast, the nanoparticles showed two peaks in all tissues except the kidney, a finding that is consistent with first-order absorption of two paclitaxel moieties, free and nanoparticle-entrapped drug. Second, because paclitaxel is mainly metabolized (30), the lower blood clearance of the total paclitaxel concentrations and the higher dose fractions of the nanoparticle formulation recovered as unchanged drug in tissues and in intestinal washings, as compared to the C/E formulation, indicate that entrapment of paclitaxel in nanoparticles retarded its metabolism. This is further confirmed by the more rapid and greater excretion of the unchanged drug into the intestinal lumen after the nanoparticles. Third, the formulation affected the specificity of paclitaxel delivery and retention in different tissues. The greatest differences were found in liver, kidneys, and small intestine where the concentrations and AUC derived from the nanoparticles were between 1.2- to 9.4-fold higher (average, 3.2 ± 2.3-fold). This finding suggests selective and preferential accumulation and retention of paclitaxel or paclitaxel-loaded nanoparticles

in these tissues. The latter is consistent with the tissue affinity of gelatin (31).

The kidneys did not show gross abnormality, for example, uneven colors as would be expected for necrotic regions, or swelling. The kidney weights also did not increase over time (less than 11% decrease over 24 h). Hence, it is unlikely that the nanoparticles obstructed the renal tubules. The mechanisms of the kidney targeting by nanoparticles are not clear and warrant further investigation.

It is noted that the total paclitaxel concentrations used in the current study represented the sum of free, protein-bound, and Cremophor micelle- or nanoparticle-entrapped paclitaxel. This might have contributed to the unusual, zigzagging drug concentration-time profiles observed in the current study. Further studies to separately measure the different drug moieties and more sophisticated kinetic models to take into account the drug release from a formulation in different tissues are needed to delineate the effects of paclitaxel formulation on its tissue pharmacokinetics and ultimately the pharmacodynamics of its antitumor activity.

In summary, results of the current study established the effects of formulating paclitaxel in nanoparticles on its clearance from blood and its distribution and retention in RES and non-RES organs. We recently reviewed the various factors and determinants of drug and macromolecule transport and delivery to and within solid tumors (32). Solid tumors have unique features, such as leaky tumor blood vessels and defective lymphatic drainage, that promote the delivery and retention of macromolecules or particulates, a phenomenon recognized as the enhanced permeability and retention effect. This consideration together with the results of the current study indicating the tissue specificity of the gelatin nanoparticles warrants further investigations on using nanoparticles to target tumors in the kidneys, liver, and small intestines.

ACKNOWLEDGMENTS

This work was supported in part by research grants R37CA49816 and R43CA107743 from the National Cancer Institute, NIH.

REFERENCES

1. E. K. Rowinsky, M. Wright, B. Monsarrat, G. J. Lesser, and R. C. Donehower. Taxol: pharmacology, metabolism and clinical implications. *Cancer Surv.* **17**:283–304 (1993).
2. M. A. Jordan, R. J. Toso, D. Thrower, and L. Wilson. Mechanism of mitotic block and inhibition of cell proliferation by taxol at low concentrations. *Proc. Natl. Acad. Sci. USA* **90**:9552–9556 (1993).
3. P. H. Wiernik, E. L. Schwartz, J. J. Strauman, J. P. Dutcher, R. B. Lipton, and E. Paietta. Phase I clinical and pharmacokinetic study of taxol. *Cancer Res.* **47**:2486–2493 (1987).
4. L. Gianni, C. M. Kearns, A. Giani, G. Capri, L. Vigano, A. Lacatelli, G. Bonadonna, and M. J. Egorin. Nonlinear pharmacokinetics and metabolism of paclitaxel and its pharmacokinetic/pharmacodynamic relationships in humans. *J. Clin. Oncol.* **13**:180–190 (1995).
5. C. M. Kearns, L. Gianni, and M. J. Egorin. Paclitaxel pharmacokinetics and pharmacodynamics. *Semin. Oncol.* **22**:16–23 (1995).
6. B. Monsarrat, P. Alvinerie, M. Wright, J. Dubois, F. Gueritte-Voegelein, D. Guenard, R. C. Donehower, and E. K. Rowinsky. Hepatic metabolism and biliary excretion of Taxol in rats and humans. *J. Natl. Cancer Inst. Monogr.* 39–46 (1993).
7. T. Walle, U. K. Walle, G. N. Kumar, and K. N. Bhalla. Taxol metabolism and disposition in cancer patients. *Drug Metab. Dispos.* **23**:506–512 (1995).
8. R. B. Weiss, R. C. Donehower, P. H. Wiernik, T. Ohnuma, R. J. Gralla, D.L. Trump, J. R. Baker Jr, D. A. Van Echo, D. D. Von Hoff, and B. Leyland Jones. Hypersensitivity reactions from taxol. *J. Clin. Oncol.* **8**:1263–1268 (1990).
9. I. Knemeyer, M. G. Wientjes, and J. L. Au. Cremophor reduces paclitaxel penetration into bladder wall during intravesical treatment. *Cancer Chemother. Pharmacol.* **44**:241–248 (1999).
10. B. Damascelli, G. Cantu, F. Mattavelli, P. Tamplenizza, P. Bidoli, E. Leo, F. Dosio, A. M. Cerrotta, G. Di Tolla, L. F. Frigerio, F. Garbagnati, R. Lanocita, A. Marchiano, G. Patelli, C. Spreafico, V. Ticha, V. Vespro, and F. Zunino. Intraarterial chemotherapy with polyoxyethylated castor oil free paclitaxel, incorporated in albumin nanoparticles (ABI-007): phase II study of patients with squamous cell carcinoma of the head and neck and anal canal: preliminary evidence of clinical activity. *Cancer* **92**:2592–2602 (2001).
11. F. D. Kolodgie, M. John, C. Khurana, A. Farb, P. S. Wilson, E. Acampado, N. Desai, P. Soon-Shiong, and R. Virmani. Sustained reduction of in-stent neointimal growth with the use of a novel systemic nanoparticle paclitaxel. *Circulation* **106**:1195–1198 (2002).
12. J. O'Shaughnessy, S. Tjulandin, N. Davidson, H. Shaw, N. Desai, M. J. Hawkins, and W. J. Gradishar. ABI-007 (ABRAXANE™), a nanoparticle albumin-bound (nab) paclitaxel demonstrates superior efficacy vs taxol in MBC: a phase III trial. *Breast Cancer Res. Treat.* **82**(Suppl 1):44 (2003).
13. N. K. Ibrahim, N. Desai, S. Legha, P. Soon-Shiong, R. L. Theriault, E. Rivera, B. Esmaeli, S. E. Ring, A. Bedikian, G. N. Hortobagyi, and J. A. Ellerhorst. Phase I and pharmacokinetic study of ABI-007, a Cremophor-free, protein-stabilized, nanoparticle formulation of paclitaxel. *Clin. Cancer Res.* **8**:1038–1044 (2002).
14. N. P. Desai, L. Louie, N. Ron, S. Magdassi, and P. Soo-Shiong. Protein-based nanoparticles for drug delivery of paclitaxel. *Trans. World Biomater. Congr.* **1**:199 (2000).
15. *Physicians' Desk Reference: PDR*. 56th ed. Medical Economics Co., 2002.
16. Z. Lu, T. K. Yeh, M. Tsai, J. L. Au, and M. G. Wientjes. Paclitaxel-loaded gelatin nanoparticles for intravesical bladder cancer therapy. *Clin. Cancer Res.* **10**:7677–7684 (2004).
17. J. J. Marty, R. C. Oppenheim, and P. Speiser. Nanoparticles–a new colloidal drug delivery system. *Pharm. Acta Helv.* **53**:17–23 (1978).
18. R. C. Oppenheim, J. J. Marty, and N. F. Stewart. Nanoparticles. *Aust. J. Pharm. Sci.* **7**:113–117 (1978).
19. D. Song and J. L. Au. Isocratic high-performance liquid chromatographic assay of taxol in biological fluids and tissues using automated column switching. *J. Chromatogr., B, Biomed. Appl.* **663**:337–344 (1995).
20. B. Davies and T. Morris. Physiological parameters in laboratory animals and humans. *Pharm. Res.* **10**:1093–1095 (1993).
21. A. Sparreboom, O. van Tellingen, W. J. Nooijen, and J. H. Beijnen. Tissue distribution, metabolism and excretion of paclitaxel in mice. *Anticancer Drugs* **7**:78–86 (1996).
22. C. Li, R. A. Newman, Q. P. Wu, S. Ke, W. Chen, T. Hutto, Z. Kan, M. D. Brannan, C. Charnsangavej, and S. Wallace. Biodistribution of paclitaxel and poly(L-glutamic acid)-paclitaxel conjugate in mice with ovarian OCa-1 tumor. *Cancer Chemother. Pharmacol.* **46**:416–422 (2000).
23. J. L. Au, D. Li, Y. Gan, X. Gao, A. L. Johnson, J. Johnston, N. J. Millenbaugh, S. H. Jang, H. J. Kuh, C. T. Chen, and M. G. Wientjes. Pharmacodynamics of immediate and delayed effects of paclitaxel: role of slow apoptosis and intracellular drug retention. *Cancer Res.* **58**:2141–2148 (1998).
24. S. J. Douglas, S. S. Davis, and L. Illum. Nanoparticles in drug delivery. *Crit. Rev. Ther. Drug Carr. Syst.* **3**:233–261 (1987).
25. V. Lenaerts, J. F. Nagelkerke, T. J. Van Berkel, P. Couvreur, L. Grislain, M. Roland, and P. Speiser. *In vivo* uptake of polyisobutyl cyanoacrylate nanoparticles by rat liver Kupffer, endothelial, and parenchymal cells. *J. Pharm. Sci.* **73**:980–982 (1984).

26. L. H. Ketai, B. A. Muggenberg, G. L. McIntire, E. R. Bacon, R. Rosenberg, P. E. Losco, J. L. Toner, K. J. Nikula, and P. Haley. CT imaging of intrathoracic lymph nodes in dogs with bronchoscopically administered iodinated nanoparticles. *Acad. Radiol.* **6**:49–54 (1999).
27. T. Yoshioka, M. Hashida, S. Muranishi, and H. Setaki. Specific delivery of Mitomycin C to the liver, spleen and lung: nano- and microspherical carrier of gelatin. *Int. J. Pharm.* **81**:131–141 (1981).
28. A. Sparreboom, O. van Tellimgem, W. J. Nooijen, and J. H. Beijnen. Preclinical pharmacokinetics of paclitaxel and docetaxel. *Anticancer Drugs* **9**:1–17 (1998).
29. A. N. Weaver, C. T. Mccarver, and H. G. Swann. Distribution of blood in the functional kidney. *J. Exp. Med.* **104**:41–52 (1956).
30. H. A. Bardelmeijer, I. A. Oomen, M. J. Hillebrand, J. H. Beijnen, J. H. Schellens, and O. van Tellingen. Metabolism of paclitaxel in mice. *Anticancer Drugs* **14**:203–209 (2003).
31. T. Yamaoka, Y. Tabata, and Y. Ikada. Body distribution of intravenously administered gelatin with different molecular weights. *J. Control. Release* **31**:1–8 (1994).
32. S. H. Jang, M. G. Wientjes, D. Lu, and J. L. Au. Drug delivery and transport to solid tumors. *Pharm. Res.* **20**:1337–1350 (2003).